# A randomized multiplex CRISPRi-Seq approach for the identification of critical combinations of genes

Nicole A. Ellis[1], Kevin S. Myers[2,3], Jessica Tung[1], Anne Davidson Ward[1], Kathryn Johnston[1], Katherine E. Bonnington[1], Timothy J. Donohue[2,3,4], Matthias P. Machner[1*]

[1]Eunice Kennedy Shriver National Institute of Child Health and Human Development, National Institutes of Health, Bethesda, Maryland, USA
[2]Great Lakes Bioenergy Research Center, University of Wisconsin-Madison, Madison, Wisconsin, USA
[3]Wisconsin Energy Institute, University of Wisconsin-Madison, Madison, Wisconsin, USA
[4]Department of Bacteriology, University of Wisconsin-Madison, Madison, Wisconsin, USA
*corresponding author: machnerm@nih.gov

## Abstract

Identifying virulence-critical genes from pathogens is often limited by functional redundancy. To rapidly interrogate the contributions of combinations of genes to a biological outcome, we have developed a multiplex, randomized CRISPR interference sequencing (MuRCiS) approach. At its center is a new method for the randomized self-assembly of CRISPR arrays from synthetic oligonucleotide pairs. When paired with PacBio long-read sequencing, MuRCiS allowed for near-comprehensive interrogation of all pairwise combinations of a group of 44 *Legionella pneumophila* virulence genes encoding highly conserved transmembrane proteins for their role in pathogenesis. Both amoeba and human macrophages were challenged with *L. pneumophila* bearing the pooled CRISPR array libraries, leading to the identification of several new virulence-critical combinations of genes. *lpg2888* and *lpg3000* were particularly fascinating for their apparent redundant functions during *L. pneumophila* human macrophage infection, while *lpg3000* alone was essential for *L. pneumophila* virulence in the amoeban host *Acanthamoeba castellanii*. Thus, MuRCiS provides a method for rapid genetic examination of even large groups of redundant genes, setting the stage for application of this technology to a variety of biological contexts and organisms.

## Introduction

There are many examples of synergistic processes in biology, often carried out by groups of redundant proteins that perform similar functions or whose activities result in the same biological outcome[1-3]. For example, the *Pseudomonas aeruginosa* genome encodes a total of 40 proteins for cyclic-di GMP synthesis and hydrolysis[4], *Legionella pneumophila* encodes 22[5], and *Vibrio cholerae* encodes at least 11[6]. Genes encoding proteins of similar function are commonly acquired either through gene duplication events or horizontal gene transfer and may have been selected for to provide fail safes to vital processes. While these redundancies generally provide benefits to the organism, they are obstacles towards gaining a fundamental understanding of biological processes. In these scenarios, the disruption of a single gene does not produce a detectable growth defect, hindering further biochemical and molecular analyses.

To dissect biological processes with intrinsic redundancy, genetic approaches must be multiplexed, allowing more than one gene to be disrupted at a time. In less tractable organisms, performing traditional deletion of individual genes, let alone combinations of genes, is laborious and time consuming. Newer genetic technologies, such as clustered regularly interspaced short palindromic repeats (CRISPR)-Cas technologies allow for fast, targeted, and multiplexed gene silencing or disruption[7, 8]. Developed from naturally occurring bacterial adaptive immune systems, CRISPR-Cas technologies are generally composed of a protein or group of proteins with enzymatic activity, usually nuclease activity, and CRISPR RNAs (crRNAs) yielding target gene specificity *via* homologous base pairing[9, 10]. *Streptococcus pyogenes* Cas9 is the most commonly used nuclease enzyme that, when guided by a crRNA to a complementary target DNA location, introduces a double-strand break[11, 12]. A catalytically inactive version of Cas9, dCas9, still localizes to complementary target genes upon crRNA direction, but instead of

56 inducing a double-strand break, precludes RNA polymerase activity, effectively silencing gene
57 expression. This gene silencing approach, referred to as CRISPR interference (CRISPRi), is most
58 effective upon binding the 5' region of the gene and is often used when a biological system lacks
59 the machinery to repair double-strand breaks produced by the original Cas9 – as is true for most
60 bacterial organisms[13, 14].

61 While silencing individual genes by CRISPRi has been achieved in various bacterial
62 species[15, 16], suppressing two or more genes simultaneously by CRISPRi has remained a major
63 challenge as it requires the expression of multiple gene-specific crRNAs. In nature, crRNAs are
64 encoded by spacers separated by identical repeats in long stretches of DNA known as CRISPR
65 arrays. Customizing CRISPR arrays in the laboratory has been a daunting task as repeat-
66 containing DNA elements are often refractory to *in vitro* synthesis and cloning. Recently, we
67 succeeded in building a multiplex CRISPRi platform in *L. pneumophila* that uses synthetic arrays
68 capable of silencing up to ten bacterial genes at a time[17]. Despite much progress, a major short-
69 coming of this and other existing multiplex CRISPRi approaches is their dependency on
70 synthesis pipelines creating arrays of a defined set of crRNA-encoding spacers that target a
71 predetermined set of genes[18-25]. In cases where predictions about the number and function of
72 genes involved in a biological process are absent or incomplete, simultaneous gene silencing by
73 CRISPRi will fail to detect synthetic lethal combinations of genes as the redundant genes not
74 targeted by the array remain functional. This emphasizes the need for a protocol for randomized
75 assembly of crRNA-encoding spacers into expansive libraries of diverse CRISPR arrays for
76 unbiased probing of varied combinations of genes. Here, we develop a multiplex, randomized
77 CRISPR interference sequencing (MuRCiS) approach that, when used in a proof-of-concept

experiment, discovered synthetic lethal combinations of genes from the virulence factor arsenal of *L. pneumophila,* the causative agent of Legionnaires' pneumonia[26, 27].

## Results

### Pre-determined CRISPR arrays fail to detect virulence-critical gene combinations

*L. pneumophila* is a Gram-negative bacterium that encodes over 300 predicted virulence factors[28, 29], known as effectors. The effectors are translocated *via* the Dot/Icm Type IV secretion system into either the natural host, free-living amoeba, or the disease host, human alveolar macrophages, to manipulate cellular processes and establish an intracellular replication compartment known as the *Legionella*-containing vacuolar (LCV)[30-32]. The study of *L. pneumophila* pathogenesis has been hindered by both the sheer number of effectors amassed by this pathogen[28, 29] and the apparent redundancy amongst them, as illustrated in the lack of detectable growth defects upon disruption of individual or even entire chromosome islands of effector-encoding genes[33, 34].

Since our earlier studies had shown that silencing of up to ten genes by multiplex CRISPRi is achievable in *L. pneumophila*[17], we built a library of 10-plex CRISPRi constructs (Table S1, MC, multiplex CRISPRi) capable of silencing more than 150 effector-encoding genes in groups of ten. The grouping of crRNA-encoding spacers into synthetic CRISPR arrays occurred based on two criteria: predicted protein function (groups 1-13, Table S1) and evolutionary conservation (groups A-D, Table S1). While evolutionary conservation was determined based on genome sequencing data from more than 38 *Legionella* species[28], protein functions were determined based on *in silico* predictions using Hidden Markov Model (HMM)-HMM-comparisons (HHPred; MPI Bioinformatics Toolkit)[35] and transmembrane predictors

101 (TMHMM)[36]. The rational was that the more conserved a gene is, the more important its
102 biological role will be and the higher the likelihood that its silencing, either alone or in
103 combination, will attenuate intracellular growth. Likewise, proteins of similar function, such as
104 two effectors with kinase activity, are likely to be redundant due to a partial overlap in their
105 range of host targets. To confirm the efficacy of multiplex gene silencing of these groups of
106 genes, we used quantitative polymerase chain reaction (qPCR) to assess knockdown efficiency
107 of gene expression by six of the seventeen MC constructs in *L. pneumophila* bearing a
108 chromosomal insertion of *S. pyogenes dcas9* at the *thyA* locus (Lp02(*dcas9*)[17]). We found that
109 10-plex gene silencing was reproducible for each construct and nearly all genes were knocked
110 down at least 2-fold, with an average fold repression of one order of magnitude or more (Figure
111 1A).

112 Upon performing intracellular growth assays with this Lp02(*dcas9*) MC strain library in
113 both U937 human macrophages and the amoeba *Acanthamoeba castellanii*, we were surprised to
114 find only a few intracellular growth phenotypes (Figure 1B). In U937 macrophages, the strains
115 containing the MC-A array caused a growth defect, which was expected since it encoded
116 crRNAs against *lpg2815* (MavN) and *lpg2300*, core effectors known to be vital for intracellular
117 growth[28]. MC-10 improved growth of Lp02(*dcas9*) in U937 cells, likely due to the silencing of
118 several glucosyltransferase effectors, *lpg1368* (Lgt1), *lpg2862* (Lgt2), and *lpg1488* (Lgt3),
119 previously shown to act in a redundant fashion[37]. MC-B caused a detectable growth defect of
120 Lp02(*dcas9*) in U937 macrophages, suggesting it had silenced one or more virulence-critical
121 effectors that had not been described before. Surprisingly, growth of the Lp02(*dcas9*) MC strain
122 library in *A. castellanii* yielded no notable phenotypes. Thus, the hypothesis that *L. pneumophila*
123 pathogenesis would be disrupted upon silencing groups of genes encoding similar or highly

conserved proteins was an oversimplification, and that redundancy reached beyond the boundary of conservation or like-function. In total, these results show that silencing a predetermined set of even 10 effector-encoding genes does not guarantee detection of synthetic lethal combinations of effectors.

**Self-assembly of a randomized multiplex CRISPR array library**

To screen for synthetic lethality more comprehensively, we developed a protocol where CRISPR arrays were assembled *de novo* from oligonucleotide pairs containing crRNA-encoding spacers. Since each spacer is flanked by 36 base pair (bp) repeats of identical sequence in a canonical CRISPR array, we rationalized that these repeat sequences could be split and then re-linked during CRISPR array assembly. As such, we designed complementary DNA oligonucleotides, which we call R-S-Rs (repeat-spacer-repeat), composed of a 24 bp spacer flanked by the terminal 12 bps of the upstream repeat and the starting 20 bps of the downstream repeat, each with four bp "sticky" overhangs (TGAA = a common Golden Gate cloning overhang, Figure 2A). The coming together of different R-S-R building blocks would recreate complete repeats without spurious nucleotides (12 + 20 + 4 = classic 36 bp repeat). Since the spacer sequence was buried within the repeat sequences, competitive advantage of one R-S-R over another for integration into an array should be negligeable. Furthermore, since the four bp overhangs are identical for each R-S-R, spacers can recombine into arrays of any length and any order. Precursor-crRNA cleavage sites were not necessary to be incorporated into the R-S-R building blocks as the precursor-crRNA would be processed into individual crRNAs by RNases endogenous to *L. pneumophila.*

146 As targets, we chose a total of 44 genes predicted to encode *L. pneumophila* effectors
147 with single or multiple transmembrane domains that were identified in the above mentioned *in*
148 *silico* prediction. These 44 transmembrane effectors (TMEs) are likely incorporated either into
149 the membrane of the LCV or that of surrounding organelles to regulate membrane dynamics or
150 the transport of metabolites (nutrients or waste products) across the membrane (Figure S1, Table
151 S2). Such TMEs, when absent due to gene silencing, are unlikely to be replaced by cytosolic
152 effectors, suggesting that redundancy is more likely to be detectable within this group of TMEs.
153 And since transmembrane regions can be predicted with high confidence, we decided to probe
154 this group of genes for synthetic lethality with the randomized CRISPRi approach as proof-of-
155 concept.
156 Assembly of CRISPR arrays followed simple, canonical cloning procedures. CRISPR
157 arrays were allowed to self-assemble after brief heat-denaturation and slow cooling of 44
158 complementary R-S-R oligonucleotide pairs with an aliquot of the "dead end" oligonucleotide
159 pairs, attB4r-R and R-attB3r (Figure 2B), to cap arrays on either end (Figure 2C). Assembled
160 arrays were locked into place by treatment with T4 ligase and incorporated into an interim
161 Invitrogen Gateway cloning plasmid, pDonorP4r-P3r, by way of the attB4r/attB3r sequences.
162 At this point, we found it critical to size-select arrays, as shorter fragments of only one or
163 two spacers efficiently out-competed longer fragments for vector incorporation, a common
164 phenomenon of basic cloning. Size-selection proved challenging (Supplemental Note S1) but
165 was ultimately accomplished through restriction enzyme-based excision of the arrays from the
166 interim plasmid and DNA gel purification of arrays of a desired size. To select for intermediate
167 (2-4 spacers) and long (4+ arrays) arrays, gel fragments corresponding to 550-650 bps and 650-

168 800 bps were purified, respectively. Purified arrays were than ligated back into the interim
169 Invitrogen Gateway cloning plasmid.
170 Lastly, we used an Invitrogen Multisite Gateway Pro cloning strategy to create a final
171 vector containing the tracrRNA-encoding sequence, and the pooled, size-selected randomized
172 CRISPR array library flanked by a promoter ($P_{tet}$) and terminator (*rrnB* T1) sequence. Keeping
173 the tracrRNA separate from crRNAs, unlike in single guide (sg)RNAs, kept the R-S-R building
174 blocks at a manageable length. Upon navigating this assembly protocol twice, the final vector
175 libraries were introduced into Lp02(*dcas9*) by electroporation and advanced to the next stage.
176
177 **Self-assembled CRISPR arrays are diverse in length, order, and composition**
178 To assess the diversity of array composition, CRISPR array-containing vector libraries
179 (Library 1 and 2) were harvested from two Lp02(*dcas9*) subpopulations, linearized, and analyzed
180 by next-generation sequencing. Importantly, given the repetitive nature of the CRISPR arrays,
181 canonical short-read sequencing technologies (such as Illumina or 454 sequencing) would not
182 have been adequate as they would not have provided enough unique sequence overlap outside of
183 the repeat sequence to map the reads back to a specific array within the mixed vector population.
184 Instead, we made use of a high-throughput, low error rate long-read sequencing technology
185 (PacBio Sequel). The average length of reads containing R-S-R elements was ~10,400 bp,
186 correlating to the size of the vector backbone plus a multiplex array (sequencing metrics reported
187 in Table S3).
188 We harvested vectors four times from each Library 1 and Library 2 stock to assess array
189 diversity and library reproducibility. We designed a custom bioinformatics pipeline (discussed
190 below) to condense data from all arrays with identical spacer content into one data set, regardless

of spacer order; as such we found that Library 1 contained 784 unique spacer combinations and Library 2 contained 1251 unique spacer combinations (overlap = 250 combinations found in both). When requiring a stringent arbitrary cut-off of five or more raw (pre-sequence-depth normalized) read counts per spacer combination, a total of 231 and 519 spacer combinations were observed in Library 1 and 2, respectively, with 121 and 300 of those spacer combinations being present in each of the four replicates (A-D and E-H; Figure 3A). We found that arrays of spacers were most often 2- to 3-plex in nature, though some reached 5-, 6-, or even up to 11-plex to give an average of 3.3 spacers per array (Figure 3B, Table S4).

Each library contained a diversity of arrays that would assess silencing of nearly all 946 possible pairwise combinations of the 44 TME genes. Chord diagrams plotting each time spacers targeting two different TME genes were found in the same array provided a visualization of the remarkable pairwise comprehensiveness of each library, with the weight of the linking lines indicating frequency of observation (Figure 3C). Both libraries showed vast diversity in array composition, with Library 2 showing the greatest randomization of arrays leading to the most comprehensive pairwise coverage. Library 1, surprisingly, had an over-representation of arrays targeting the same five genes (*lpg0963, lpg2223, lpg2552, lpg2888,* and *lpg3000)* that accounted for 20% of all arrays in that library (indicated by the thick network of linking lines). Notably, from an array building vantage, the 5-plex arrays targeting these five genes were found to have seven different spacer orders, indicating that they had been randomly generated multiple times during the assembly step.

Lastly, we examined the overall abundance of each spacer in the libraries to verify that no one crRNA-encoding spacer was individually toxic, that is, targeting a gene essential for *L. pneumophila* axenic growth (intended or off-target). When combining data from all libraries,

214 each spacer was present a median of ~5328 times (Figure S2). No one spacer was under-
215 represented, confirming none was toxic, but also that each R-S-R element had an equal
216 opportunity to be incorporated in an array. Together, these two libraries provide a vast collection
217 of multiplex arrays to test for combinatorial TME gene contributions to *L. pneumophila*
218 pathogenesis strategies.
219
220 **Decoding randomized CRISPR array libraries by high-throughput sequencing**
221 To identify combinations of genes that, upon silencing, were detrimental to intracellular
222 *L. pneumophila* replication, vectors from Lp02(*dcas9*) cultures bearing the pooled input array
223 libraries were purified, linearized, and PacBio Sequel-sequenced to determine the identity and
224 composition of arrays before infection (Figure 4A). From the same cultures, pooled bacteria
225 were simultaneously introduced to a selective pressure, in this case host cell infection, and
226 surviving bacteria were harvested from host cells after 72 h (for U937 macrophage infections) or
227 48 h (*A. castellanii* infections) and grown as single colonies on media plates. Vectors from
228 arising bacterial colonies were purified, linearized, and analyzed again by long-read sequencing
229 to determine the identity of arrays in the output vector pool.
230 Since each PacBio sequencing read reported the complete spacer composition of an array,
231 barcoding was unnecessary. A custom read count-based bioinformatics pipeline was designed to
232 determine arrays that were under-represented in the output pool, and therefore, must have
233 silenced genes vital for successful intracellular replication (Figure 4B,
234 https://github.com/GLBRC/MuRCiS_pipeline). Taking a most stringent approach, only reads
235 that were an exact match to the repeat sequence were analyzed. Spacers within an array were
236 identified by searching each read for exact matches to all possible forward and reverse

combinations of spacer sequences and the repeat sequence. The number of arrays with the same spacer composition were counted and an arbitrary cut-off of five raw counts in the input pool was required for further analysis of that unique spacer combination. The remaining unique array counts were normalized for run-to-run sequence depth variation, and the proportion of each unique array compared to the total number of sequenced reads containing a repeat sequence was determined for each sample. For each experiment, the proportion of normalized counts for each unique spacer composition in the input sample was compared to the normalized counts for the same spacer composition in the output sample to determine a fold reduction. The larger the reduction, the more disadvantageous silencing of the targeted genes was for intracellular *L. pneumophila* replication. We excluded any subset of spacers with an input *vs.* output reduction of less than five-fold. Together, this experimental and bioinformatics pipeline forms the basis for MuRCiS.

**MuRCiS elucidates novel combinations of virulence-critical genes**

We first interrogated the contributions of TME genes to successful intracellular replication of *L. pneumophila* in human U937 macrophages. We performed four rounds of infections: two with Lp02(*dcas9*) bearing Library 1 (U-1A and U-1B) and two with Lp02(*dcas9*) bearing Library 2 (U-2A and U-2B). Each pair of infections, A and B, occurred independently of each other serving as biological replicates. To test technical reproducibility, we also collected output samples twice (T1 and T2) when performing experiments "A". The four inputs for these experiments were A, C, E, and G (Figure 3A). In total, the four input cultures used to challenge U937 macrophages allowed for the probing of 710 of a possible 946 pairwise combinations (75%) of 44 TME when requiring a stringent arbitrary cut-off of five or more raw read counts

(Figure 5A, Table S4). In fact, pairs were often in the input pool between eleven and 500 times allowing for in-experiment replication. Silencing *mavN,* which encodes the essential metal ion transporter, served as a control for the infection experiments. While hundreds to thousands of reads bearing the crRNA$^{mavN}$-encoding spacer were present in each input pool, each of the output samples (T1/T2 summed) had only ten or fewer reads (Figure 5B). These results indicated that MuRCiS could identify virulence-critical genes by monitoring changes in spacer abundance during host cell infection.

In total, 641 unique spacer combinations with five or more raw input reads were tested using this protocol (Figure 5C). Subsequent bioinformatic analyses found that 231 of those combinations showed a five-fold or greater reduction in read counts. All 59 combinations which contained the crRNA$^{mavN}$-encoding spacer were removed from the list, and 39 spacer combinations were identified as having a five-fold or greater read count reduction in both replicates of each library experiment (including both technical replicates). These 39 spacer combinations were examined further by gathering shorter versions of the arrays to track down the minimal number of spacers needed for the strain to show a fitness defect (Table S5). Twenty critical combinations of spacers were identified, of which most were 2- to 3-plex combinations (Figure 5D and 5E). Because of the uniqueness of Libraries 1 and 2, different gene combinations were discovered by each library to be virulence-critical, suggesting that the assembly and assay of more than one library was advantageous for comprehensiveness. Targeting of *lpg2888* and *lpg3000* was identified to be deleterious to *L. pneumophila* intracellular growth in experiments with both libraries. Table S6 shows data for each of the subsets of the 20 critical gene combinations, providing evidence that it was truly the silencing of the reported combination of genes, and not fewer or individual genes, that was needed for strain to show a fitness defect.

**Multiple TME pairs are critical for *L. pneumophila* virulence in macrophages**

The nature of CRISPRi gene silencing and the novelty of the screen performed here mandated confirmation of targets by construction of strains with true chromosomal gene deletions, as the degree of target silencing can be influenced by a range of factors related to (1) crRNA design, (2) genetic environment, and on occasion (3) off-target effects. Individual and pairwise deletions of the candidate genes were made for five of the combinations identified in Figure 5E. All deletion strains were whole genome sequenced for confirmation of gene deletion and absence of background mutations and then used to challenge macrophages. Their ability to survive and grow over a period of three days was determined by plating assay.

This analysis confirmed the expected growth-inhibitory phenotype for three of the five gene pair deletions (Figure 5F), namely *lpg2888-lpg3000*, *lpg1959-lpg2804*, and *lpg0096-lpg2804*. The severity of the phenotype varied amongst the different pairs, ranging from a ~75-fold reduction in growth to complete inability to replicate in the host. For two pairs, *lpg2552-lpg3000* and *lpg0096-lpg2888*, we found that deleting only one of the genes, *lpg3000* and *lpg2888*, respectively, was sufficient for limiting *L. pneumophila* intracellular replication (Figure 5G). While we aimed to find critical combinations of genes, these “false positive hits” still identified genes important to *L. pneumophila* intracellular replication demonstrating much can be learned from this assay.

**Virulence-critical gene combinations are host-specific**

Having found critical combinations of genes required for growth of *L. pneumophila* in its disease host, we next interrogated the cohort of TME genes for their necessity during *L.*

306 *pneumophila* growth in the natural host, *A. castellanii*. As before, we performed four rounds of
307 infections: two with Lp02(*dcas9*) bearing Library 1 (AC-1A and AC-1B) and two with
308 Lp02(*dcas9*) bearing Library 2 (AC-2A and AC-2B). The four inputs for these experiments were
309 B, D, F, and H (Figure 3A). In total, these four inputs allowed for probing 672 of a possible 946
310 pairwise combinations (71%) of 44 TME genes when requiring a stringent arbitrary cut-off of
311 five or more raw read counts (Figure 6A, Table S4).

312 This time, 571 unique spacer combinations with five or more raw input reads were tested
313 during the experiments, leading to the identification of 71 spacer combinations with five-fold or
314 greater reduction in read counts (Figure 6B). Of those, 21 emerged from both replicates of a
315 given library experiment. We examined these spacer candidates further by tracking the most
316 minimal number of spacers needed to attenuate *L. pneumophila* intracellular growth (Table S7).
317 Six critical combinations of TME genes were ultimately identified, of which all were 2-plex
318 combinations (Figure 6C and 6D, Table S8). Notably, silencing of *lpg2888* and *lpg3000* was
319 again found to be deleterious to *L. pneumophila* growth in *A. castellanii,* as it was in U937
320 macrophages (Figure 5E). Having already constructed *L. pneumophila* stains bearing deletions in
321 *lpg2888* and/or *lpg3000*, we tested these for growth in *A. castellanii.* Surprisingly, in *A.*
322 *castellanii* deletion of *lpg3000* alone was sufficient to cause a growth defect as dramatic as that
323 observed for the double mutant (Figure 6E). This contrasted with U937 macrophage experiments
324 where only deletion of both *lpg2888* and *lpg3000* resulted in attenuated growth (Figure 5F).

325 Two of the other critical virulence-gene combinations identified in the *A. castellanii*
326 experiments also contained *lpg3000: lpg0086-lpg3000* and *lpg0621-lpg3000,* suggesting we
327 would again observe deletion of *lpg3000* sufficient of a maximum intracellular growth defect if
328 tested. Though each library included 1-plex arrays expressing only crRNA$^{lpg3000}$ for silencing

329 *lpg3000*, we did not identify those 1-plex arrays as being sufficient to attenuate virulence, likely
330 because their decrease was not consistent between Library 1 and Library 2 experiments, although
331 there was consistency between replicates A and B of each library (Table S8). A possible
332 explanation was that incomplete knockdown (*vs.* complete knockout) of a seemingly important
333 process was at a tipping point of phenotype extremes, and that silencing of an additional effector
334 may have tipped the scale. If requiring a five-fold or greater reduction in only one library and not
335 the other, an additional three (two of which are 1-plex; *lpg0086* and *lpg2223*) and six (one of
336 which is 1-plex; *lpg0086*) spacer combinations may qualify as critical to U937 macrophage and
337 *A. castellanii* infection, respectively.
338
339 **Single-round CRISPRi experiments are of sufficient sensitivity to detect virulence-critical**
340 **genes**
341 For any virulence-critical gene combination to be listed as hit during U937 macrophages
342 infection (Figure 5) or *A. castellanii* infection (Figure 6), the CRISPR arrays silencing them had
343 to pass the most stringent cutoff criteria, including that the spacer combination had to be
344 represented in both biological replicates, A and B. There were instances though where CRISPR
345 arrays were reduced in only one replicate because arrays bearing the same spacer combinations
346 were absent in the other replicate (input overlap shown in Figure 3A). When requiring a five-fold
347 or greater reduction in only one replicate, an additional 18 and 14 virulence-critical spacer
348 combinations were observed in the U937 macrophage and *A. castellanii* experiments,
349 respectively (Table S9). For example, in the infection experiment AC-2A, arrays silencing both
350 *lpg0096* and *lpg2888* were nine-fold under-represented in the output pool after *L. pneumophila*
351 growth in *A. castellanii*. *L. pneumophila* strains bearing deletions in either one or both genes

were examined for growth in *A. castellanii*. Interestingly, unlike in U937 macrophages, we did observe a synergistic phenotype upon deletion of *lpg0096* and *lpg2888* (Figure 6F). These data represent yet another example of a host-specific phenotype and suggest that the proof-of-concept study performed here may have identified even more virulence-critical combinations of *L. pneumophila* genes than initially thought warranting examination of gene combinations that are considered hits in only one of the experimental replicates.

**Discussion**

In this study, we expanded the versatility of CRISPRi platforms in bacteria by devising an approach capable of "shuffling" the spacer composition of CRISPR arrays, thus creating a randomized, multiplexed genetic tool adept to cross-examine even large cohorts of *L. pneumophila* effectors for synthetic lethality. A critical innovation of our approach was the quantitative (abundance output vs input pool) and qualitative (spacer composition) analysis of CRISPR arrays by high-throughput long-read sequencing. Indubitably, MuRCiS will be applicable to the study of any group of redundant genes in a wide range of CRISPRi-capable organisms.

Our *de novo* assembly protocol created distinct libraries of arrays each time it was executed, exemplifying its truly random nature (Figure 3). As mentioned, Library 1 unexpectedly amassed arrays targeting five specific genes (*lpg0963, lpg2223, lpg2552, lpg2888,* and *lpg3000)*, such that these arrays accounted for 20% of the input read counts for this library. These arrays did decrease in abundance during *L. pneumophila* infection of both U937 macrophages and *A. castellanii,* consistent with our finding that *lpg2888* and *lpg3000* are important for replication in both these hosts. We do not fully understand why these particular arrays were so prevalent only

375 in Library 1, even more so given that assembling arrays of fewer than five spacers proved more
376 efficient (Figure 3B). It is possible that silencing these TME genes provided *L. pneumophila* with
377 a fitness advantage during axenic growth causing them to be overrepresented in the input pool.
378 A unique feature of MuRCiS is its ability to quickly assign phenotypes to exact spacer
379 combinations simply by tracking phenotypes seen with longer arrays to shorter arrays with
380 subsets of spacers and, hence, target genes for subsequent follow-up studies (Table S5 and Table
381 S7). For example, the 5-plex arrays containing *lpg0963, lpg2223, lpg2552, lpg2888,* and *lpg3000*
382 can be subdivided into 30 subsets of spacers - all of which were present in the experiment and
383 allowed assigning the phenotype to just two genes, *lpg2888* and *lpg3000* (Table S5). Notably,
384 not all phenotypes caused by long arrays could be condensed to just one or two spacers. Some
385 phenotypes required 4- or 5-plex gene silencing (Table S6), showing that although only a minor
386 fraction of all possible combination of three or more spacers were represented in our array
387 library, the approach was capable of identifying these synthetic lethal gene silencing
388 combinations as well.
389 Examining the PacBio DNA sequencing data, we found that the number of unique arrays
390 identified in a given sample increased as the read number increased (Table S3). For this proof-of-
391 concept experiment we chose to limit the initial pool of arrays for analysis to those with a
392 minimum of five raw input counts. Maintaining this same cut-off with increased sequence depth
393 undoubtedly would increase the input-to-input array overlay (Figure 3A) and the
394 comprehensiveness of surveying pairwise silencing of genes (Figures 5A and 6A). We
395 anticipated the gains of increased sequencing depth by recalculating the coverage of the
396 correlation plots in Figure 5A and 6A such that the observed coverage of 710/946 (75%) or
397 672/946 (71%) pairs with the requirement of five raw input counts increased to 789/946 (83%)

398 or 782/946 (83%) pairs when the requirement was lowered to just one raw input count,
399 respectively. Hence, the ability to make comprehensive libraries was even better than first
400 reported.

401 Array length poses the biggest bottleneck to performing MuRCiS on larger groups of
402 genes. Here, each of the libraries individually probed an average of ~1000 different spacer
403 combinations (independent of order). If all spacer combinations were represented by 2-plex
404 arrays, theoretically one could investigate pairwise combinations of ~45 genes using just 990
405 arrays. But as reported, the assembly protocol produced longer arrays of up to 11 spacers,
406 averaging 3.3 spacers. Each time the average length of arrays is increased by one spacer, the
407 number of pairwise combinations able to be probed dramatically increases. If all arrays were 3-
408 plex, 3000 pairwise combinations would be possible within just 1000 arrays allowing
409 comprehensive interrogation of a group of ~75 genes for synthetic lethality, and if all arrays were
410 4-plex, 6000 pairwise combinations would be possible within just 1000 arrays allowing
411 comprehensive interrogation of a group of ~110 genes for synthetic lethality. As it stands, the
412 theoretical upper limit of MuRCiS seems between 75-100 genes, but with the construction of
413 more than one library, deeper sequencing, and lowered input count requirements this number
414 could easily be expanded.

415 Excitingly, the combinatorial effector gene deletions that were assayed in our
416 experiments produce some of the largest phenotypes yet identified pertaining to *L. pneumophila*
417 intracellular replication (Figure 5 and 6). This is especially true of the simultaneous deletion of
418 *lpg2888* and *lpg3000* producing a truly synthetic lethal phenotype during U937 macrophage
419 infection. The only other pair of *L. pneumophila* genes known to have such a large combinatorial
420 impact on *L. pneumophila* intracellular replication are *icmW* and *icmR*[41], genes that encode

421 components of the Dot/Icm Type IV secretion system itself; hence their deletion has a global
422 effect limiting translocation of many effector proteins into the host. HHpred analysis of *lpg2888*
423 revealed numerous high confidence hits to tripartite pore-forming toxin components, while
424 *lpg3000* showed high confidence hits to ABC transporter proteins. Additional studies are
425 ongoing to uncover why deletion of their encoding genes caused synthetic lethality. From an
426 evolutionary standpoint, it was interesting that synergy of these genes was only seen during *L.*
427 *pneumophila* infection of U937 macrophages. During *A. castellanii* infections, deletion of just
428 *lpg3000* was already lethal, whereas deletion of *lpg2888* alone caused only a minor growth
429 defect (Figure 6E). These data are in agreement with data from a transposon sequencing (Tn-
430 Seq)-based screen that identified a growth defect upon disruption of *lpg3000* in *L. pneumophila*
431 during infection of *A. castellanii* and another protist, *Hartmannella vermiformis*[42]. Altogether,
432 these results suggest that the biological process promoted by *lpg3000* is evolutionarily essential
433 for growth in the natural amoeban host. Clearly, MuRCiS identified exciting biology pertaining
434 to *L. pneumophila* pathogenesis; and if applied to other groups of genes, other selective
435 pressures, or other microorganisms, it undoubtedly has the potential to do the same.
436
437
438 **Methods**
439 **Strains and cell lines**
440 All *L. pneumophila* strains are listed in Table S10 and were derived from the parent strain
441 *L. pneumophila* Philadelphia-1 Lp02 (*thyA hsdR rpsL*). Host cell lines included U937 monocytes
442 (ATCC CRL-1593.2) which were differentiated into macrophages with 12-O-
443 tetradecanoylphorbol-13-acetate (TPA, Sigma-Aldrich P1585) and *A. castellanii* (ATCC 30234).

444 **Synthetic MC array construction**

445 Synthetic 10-plex MC array constructs were synthesized by GenScript and moved into
446 pMME977 (*thyA*+) by Multisite Gateway Pro cloning (Invitrogen 12537-100) as previously
447 described[17]. The MC arrays tested here bear a *boxA* sequence -58 bp upstream of the first repeat
448 which was added after vector completion by quick-change PCR as described previously[17]. Final
449 plasmids were introduced to Lp02(*dcas9*) by electroporation and the strains containing the
450 plasmids were selected for on CYE plates[43] without thymidine. Spacer composition of each array
451 and their corresponding nucleotide sequences are listed in Table S1.

452 **Axenic growth of *L. pneumophila* 10-plex CRISPRi strains**

453 As described previously[17], *L. pneumophila* cultures were grown overnight in AYE +Fe
454 +Cys (10 g ACES, 10 g yeast extract per liter, pH 6.9 with 0.4 mg/ml cysteine and 0.135
455 mg/ml ferric nitrate) under non-inducing conditions. On the second day, cultures were sub-
456 cultured twice (AM and PM, ~6-7 h apart) to OD600 0.2–0.3 with 2–3 mL fresh AYE +Fe +Cys
457 containing 40 ng/mL anhydrous tetracycline (aTC, Clontech 631310). On the third day, cultures
458 that had reached OD600 3-5 (post-exponential growth) were collected for mRNA analyses
459 and/or used in host cell infections.

460 **RNA extraction and qPCR**

461 RNA extraction was performed on bacteria pellets after aTC induction using the Trizol
462 Max Bacterial RNA Isolation Kit (Invitrogen 16096040). Contaminating DNA was removed
463 using the Turbo DNA-free Kit (Invitrogen AM1907) and RNA was converted to cDNA using the
464 High-Capacity cDNA Reverse Transcription Kit (Applied Biosystems 4368814). qPCR was
465 performed using the SYBR Green Master Mix (Applied Biosystems 4367659) on a StepOne Plus
466 Real-Time PCR System (Applied Biosystems) using comparative CT. qPCR primers are listed in

467 Table S1. mRNA levels from different samples were normalized to a house-keeping gene (*rpsL*)
468 and mRNA levels in CRISPRi strains were compared to that of a vector-bearing Lp02(*dcas9*)
469 control strain using the ΔΔCT method[44] to determine fold repression.

470 **CRISPRi intracellular growth assays**

471 U937 monocytes (ATCC CRL-1593.2) were maintained in DMEM (Mediatech 15-013-
472 CV) + 10% FBS + glutamine at 37 °C. Two days prior to challenge with *L. pneumophila*, cells
473 were plated on 24-well plates at $3x10^5$ cells/well with 0.1 µg/mL 12-O-tetradecanoylphorbol-13-
474 acetate (TPA, Sigma-Aldrich P1585) to promote differentiation. *L. pneumophila* strains bearing
475 each MC array were incubated under inducing conditions, as described above, and added to
476 differentiated U937 macrophages in DMEM + 10% FBS + glutamine containing 40 ng/mL aTC
477 at a multiplicity of infection (MOI) of 0.05. Plates were centrifuged for five minutes at 200 x g to
478 increase bacteria-macrophage contact. After a 2 h incubation at 37 °C, extracellular bacteria were
479 removed by washing the macrophages twice with DMEM + FBS + glutamine media containing
480 40 ng/mL aTC. Both 2 and 72 hours post infection (hpi) intracellular bacteria were collected
481 upon macrophage cell lysis by addition of digitonin (0.02% final concentration), serially diluted,
482 and spotted on CYE plates. Results are given as fold growth (CFUs harvested 72 hpi *vs.* 2 hpi)
483 compared to that of the vector-bearing Lp02(*dcas9*) control.

484 *A. castellanii* (ATCC 30234) were maintained in PYG media[45] at 25 °C. The day before
485 challenge with *L. pneumophila*, cells were plated on 24-well plates at $3x10^5$ cells/well. The
486 morning of challenge, the media in the *A. castellanii* plates was changed from PYG to AC
487 buffer[45] to promote starvation for 2 h at 25 °C. *L. pneumophila* strains bearing each MC array
488 were incubated under inducing conditions, as described above, and added to the starved *A.*
489 *castellanii* in AC buffer containing 40 ng/mL aTC at a MOI of 0.03. Plates were centrifuged for

490 five minutes at 200 x g to increase bacteria-amoeba contact. After a 2 h incubation at 37 °C,
491 extracellular bacteria were removed by washing amoeba twice with AC buffer containing 40
492 ng/mL aTC. Both 2 and 48 hpi intracellular bacteria were collected upon amoeba lysis by
493 addition of saponin (0.05% final concentration), serially diluted, and spotted on CYE plates.
494 Results are given as fold growth (CFUs harvested 48 hpi *vs.* 2 hpi) compared to that of the
495 vector-bearing Lp02(*dcas9*) control.

496 **Multiplex random CRISPR array self-assembly protocol**

497 R-S-R oligonucleotides were designed as the building blocks for array assembly. For
498 each gene, the reverse complement of the 24 nucleotides downstream of the first PAM sequence
499 (NGG) after the transcription start site was identified and would become the spacer sequence.
500 This sequence was checked to be null of cut sites for SacI (GAGCTC), NotI-HF (GCGGCCGC),
501 and AflII (CTTAAG) as these are used for downstream steps; if not, the sequence adjacent the
502 subsequent PAM sequences was checked. Spacer sequences were then flanked on either side
503 with one half of the repeat according to the following scheme: top oligonucleotide (5' to 3'):
504 tgaatggtcccaaaac-24 nt spacer-gttttagagctatgctgttt. Bottom oligonucleotide (5' to 3'):
505 ttcaaaacagcatagctctaaaac-24 nt complement-gttttgggacca. Standard oligos were ordered from
506 Eurofins Genomics already resuspended in water at 100 μM concentration. Dead end
507 oligonucleotide pairs for R-attB4r and R-attB3r did not contain a spacer but did contain the
508 upstream or downstream repat sequence fused to the attB4r or attB3r Invitrogen Gateway
509 cloning sequence, respectively.

510 For array assembly, top and bottom oligonucleotides for a single R-S-R or dead end
511 oligonucleotide pairs were combined 1 μL:1 μL and were phosphorylated in a 50 μL reaction
512 using T4 Polynucleotide Kinase (NEB M0201L) for 2 h at 37 °C. The reaction was stopped by

513 addition of NaCl to a final concentration of 50 mM. Next, 2 μL of each phosphorylated R-S-R
514 oligonucleotide pair for all 44 gene targets and 10 μL of the dead end oligonucleotides were
515 combined in a single microcentrifuge tube. The microcentrifuge tube was placed in a heat block
516 at 95 °C for 5 minutes and then the heat block was turned off and allowed to cool to room
517 temperature for 2 h. Assembled arrays were preserved through ligation with T4 DNA ligase and
518 its corresponding buffer (NEB M0202L) for 1.5 h at room temperature. The reaction was
519 purified using a NucleoSpin PCR Clean-up Kit (Macherey-Nagel 740609.250) and eluted in 30
520 μL 1X TE buffer.

521 To size select arrays of interest, four 6.5 μL aliquots of the purified arrays were moved
522 into the interim pDonor4r-3r in parallel by the standard Invitrogen Gateway BP reaction recipe
523 (ThermoFisher 11789-020) which was allowed to remain at room temperature for 72 h prior to
524 stopping the reactions with Proteinase K and transformation of all material into *E. coli* GC5
525 (Genesee Scientific 42-650) with selection on LB+Kan (30 μg/mL) plates. All colonies were
526 scraped off plates using an inoculation loop and added directly to the A1 buffer of a Nucleospin
527 Plasmid Purification Kit (Macherey-Nagel 740499.250) for plasmid isolation and elution in
528 water. A NotI-HF (NEB R3189S) and AflII (NEB R0520S) double digest was performed on the
529 four now recombined eluates, as well as one aliquot of the circular empty pDonor4r-3r plasmid,
530 at 37 °C overnight. Next, a 1% agarose gel was used to separate the vector backbone from the
531 excised size-ordered arrays, and we collected bands containing arrays ≥2-plex at 550-650 bps
532 and 650-800 bps to be purified separately using a NucleoSpin Gel Purification Kit (Macherey-
533 Nagel 740609.250). We also collected the cut vector backbone, but only from the empty
534 pDonor4r-3r sample. For all steps forward, the 550-650 bps and 650-800 bps samples were kept
535 separate, but procedures were carried out in parallel. As such, purified arrays were ligated back

536 into the pDonor4r-3r backbone using T4 DNA ligase for 2.5 h at room temperature, all material
537 was transformed with the plasmid into *E. coli* GC5, and re-circulated plasmids were selected for
538 on LB+Kan plates. All colonies were scraped off plates using an inoculation loop and added
539 directly to the A1 buffer of a Nucleospin Plasmid Purification Kit (Macherey-Nagel 740499.250)
540 for plasmid isolation and elution in 20 μL 1X TE buffer. At this point, individual plasmids can
541 be sequenced using a primer with the sequence: GTTTTCCCAGTCACGAC, if individually
542 purified from a single colony, to confirm successful array assembly.

543 A Multisite Gateway Pro kit (Invitrogen 12537-100) was used to move arrays into the
544 final vector. To generate the promoter-bearing donor plasmid pMME2162, the *tet* promoter was
545 amplified from pMME1996 with primers containing attB5/attB4 ends for recombination into the
546 pDonorP5-P4 via a standard Invitrogen Gateway BP reaction. To generate the terminator-bearing
547 donor plasmid pMME2163, the *rrnB* T1 terminator was amplified from pMME1996 with
548 primers containing attB3/attB2 ends for recombination into the pDonorP3-P2 via a standard
549 Invitrogen Gateway BP reaction. Next, the size-selected arrays in the pDonor4r-3r plasmid were
550 combined with pMME985 (tracrDNA in pDonorP1-P5r, described previously[17]), pMME2162,
551 and pMME2163, and were added to the pMME977 destination vector (attR1/attR2, +*thyA*) by
552 using three-times the standard Invitrogen LR reaction recipe (ThermoFisher 11791-020), with
553 addition of β-mercaptoethanol to a final concentration of 1 mM, and allowed to remain at room
554 temperature for 72 h prior to stopping the reactions with Proteinase K and electroporation into *E.*
555 *coli* GC5 with selection on LB+Amp (100 μg/mL) plates. Next, all colonies (generally thousands
556 for 550-650 bps samples and hundreds for 650-800 bps samples) were scraped off plates using
557 an inoculation loop and added directly to the A1 buffer of a Nucleospin Plasmid Purification Kit
558 (Macherey-Nagel 740499.250) for plasmid isolation and elution in 20 μL water. At this point,

individual plasmids can be sequenced using a primer with the sequence: CAACCACTTTGTACAAGAAAGCTGGG, if individually purified from a single colony, to confirm successful construct assembly.

Lastly, 10 μL of these final plasmids were introduced into Lp02(*dcas9*) by electroporation and recipient cells were selected for on CYE plates. Colonies were scraped off plates using an inoculation loop, added to 15 mL AYE +Fe +Cys, vortexed, and frozen in 1 mL aliquots with glycerol (final concentration 15%) to be stored at -80 °C. Freezer stocks of Lp02(*dcas9*) bearing each of the size-selected portions of a given library (Library 1 and 2) are listed in Table S10.

**MuRCiS intracellular growth assays**

*L. pneumophila* bearing each size-selected portion of either Library 1 or 2 were patched from -80 °C freezer stocks onto CYE plates. Two days prior to infection *L. pneumophila* cultures of each were grown overnight in 3 mL AYE +Fe +Cys under non-inducing conditions. On the second day, cultures were sub-cultured twice first in the AM to OD600 0.2 with 3 mL fresh AYE +Fe +Cys containing 40 ng/mL aTC and then ~6-7 h later, to OD600 0.2 with 4 mL fresh AYE +Fe +Cys containing 40 ng/mL aTC (two cultures each). On the third day, cultures pertaining to either Library 1 or 2 were combined in one tube to serve as a single culture for infection (input vector pool). For Library 1, two different 550-650 bps portions and one 650-800 bps portion was combined. For Library 2, one 550-650 bps portion and one 650-800 bps portion was combined.

U937 monocytes were maintained in DMEM + 10% FBS + glutamine and allowed to differentiate into macrophages with 0.1 μg/mL TPA for three days prior to *L. pneumophila* challenge. *A. castellanii* were maintained in PYG and starved in AC buffer 2 h prior to challenge

with *L. pneumophila*. Ultimately, differentiated U937 macrophages or starved *A. castellanii* were plated in two to three 10 cm dishes at a density of $1x10^7$ cells per dish.

Infections were carried out with 40 ng/mL aTC in the host cell media at an MOI of 0.05 for differentiated U937 macrophages and 0.03 for starved *A. castellanii*. After addition of bacteria, the 10 cm dishes were spun down at 200 x g to increase bacteria-host cell contact and incubated for 2.5 h at 37 °C. Next, host cells were washed in their corresponding media with 40 ng/mL aTC to remove extracellular bacteria and then placed back at 37 °C for the duration of the infection, 72 h or 48 h for U937 macrophage and *A. castellanii* infections, respectively. To collect input vector pools, bacteria from the cultures used for infection were immediately pelleted by centrifugation and resuspended in 8 mL of RES-EF of the NucleoBond Xtra Midi EF kit prior to proceeding with the standard kit protocol (Macherey-Nagel 740420.50). Precipitated vectors were resuspended in 120 μL of water.

Following the infection duration, *L. pneumophila* were harvested from either the U937 macrophages or *A. castellanii* 10 cm dishes (15 mL vol) by addition of 300 μL of 1 % digitonin or 600 μL of 1% saponin, respectively. Next, 10 cm dishes were incubated for 10 minutes at 37 °C, followed by pipet agitation of the cells and collection of the media in 50 mL conical tubes. The conical tubes were shaken vigorously to promote host cell lysis and the *L. pneumophila* were pelleted by centrifugation for 10 min at 3500 x g. The resulting bacteria pellets were resuspended in a minimal amount of supernatant and plated on CYE plates. All colonies were scraped off plates using an inoculation loop and resuspended in 8 mL of RES-EF of the NucleoBond Xtra Midi EF kit prior to proceeding with the standard kit protocol for collection of the output vector pools. Precipitated vectors were resuspended in 120 μL of water.

**PacBio long-read sequencing**

604 Purified vector populations from input and output samples were linearized by addition of
605 24 µL of SacI restriction enzyme (NEB R0156L) with 16 µL of NEB r1.1 buffer and overnight
606 incubation at 37 °C. To purify the linearized vectors, the AMPureXP Bead protocol (Beckman
607 Coulter A63880) was followed using 100 µL of bead slurry. Final eluent volumes varied
608 between samples based on the ability to get a bead-free eluent. Generally, ~10 µL of water was
609 needed for input sample elution and ~40 µL of water was needed for output sample elution.
610 Input DNA concentrations were generally ~200-300 ng/uL and output DNA concentrations were
611 usually 300-700 ng/uL. Vector linearization was confirmed on a 1% agarose gel.
612 PacBio long-read sequence of the linearized vectors was performed by the NIH NICHD
613 Molecular Genomics Core. Samples were prepared for sequencing on a Sequel instrument
614 (PacBio) using the Sequencing Primer v4 and the Sequel Binding Kit 3.0. Samples were
615 multiplexed and run on multiple SMRT cells simultaneously (# SMRT cells = # multiplex
616 samples divided by 2 or 3) with 10 h of sequencing camera time.
617 **Bioinformatics pipeline**
618 PacBio sequencing files (ccs_bam files) were processed using a custom bioinformatics
619 pipeline (https://github.com/GLBRC/MuRCiS_pipeline). Total read number and lengths were
620 determined using Samtools[46] (version 1.9) and standard Linux commands (see GitHub for
621 specific commands). All spacer and repeat forward and reverse orientation sequence
622 combinations were used to identify the unique array sequence in the sequencing files using the
623 "count_spacers_NIH.py" custom Python script (https://github.com/GLBRC/MuRCiS_pipeline).
624 Reads lacking an exact match to the repeat sequence were removed from further analysis. Counts
625 for unique spacers were normalized by dividing the read count plus a pseudocount of 1 by the
626 total number of reads with repeat sequences multiplied by 10,000 in a modified Counts Per

627 Million (CPM) equation. The 10,000 value was used instead of 1 million due to the lower

628 number of overall reads from this PacBio sequencing.

$$\frac{(Read\ Count + Pseudocount) * 10{,}000}{(Total\ reads\ with\ repeat\ sequences)}$$

629

630 To determine the pairwise correlation of two spacers and plot Chord diagrams, the

631 "chord_correlation_plot_script.R" script was used. All plots were generated in R (version 4.1.0)

632 and all scripts and command descriptions are available on GitHub

633 (https://github.com/GLBRC/MuRCiS_pipeline).

634 **Deletion strain construction and whole genome sequencing**

635 *L. pneumophila* gene deletion strains were constructed using gene-specific versions of the

636 pSR47s suicide plasmid listed in Table S10 and described recently[47]. In our hands, each pSR47s

637 plasmid was introduced into the *L. pneumophila* strain background of choice with the help of

638 pRK600 by tripartite mating as described previously[48]. Successful strains were confirmed by

639 failure to grow on CYET+Kan, colony PCR, and whole genome sequencing.

640 For whole genome sequencing, genomic DNA of *L. pneumophila* was extracted using the

641 Wizard Genomic DNA Purification Kit (Promega A1120), following the standard Gram-negative

642 bacteria protocol, and resuspended in 10 mM Tris-HCl, 1 mM EDTA buffer. The Illumina

643 Nextera XT DNA Library Preparation Kit (#FC-131-1096) was used to prepare libraries for

644 sequencing on an Illumina MiSeq System by the NIH NICHD Molecular Genomics Core.

645 Nucleotide variants were called using HaplotypeCaller (version GATK3, Broad Institute).

646 Integrative Genomics Viewer (version 2.4.14, Broad Institute) was used to visually confirm

647 chromosome deletions. Final deletion strains are listed in Table S10.

648 **Deletion strain intracellular growth assays**

Intracellular growth assays with deletion strains were performed exactly as for the 10-plex CRISPRi intracellular growth assays except that U937 monocytes were allowed to differentiate for three days prior to *L. pneumophila* challenge and *L. pneumophila* cultures were simply grown overnight without the inducer aTC. To overcome the thymidine auxotrophy of Lp02 strains, thymidine at a final concentration of 0.1 mg/mL was added directly to *L. pneumophila* cultures and to the DMEM + 10% FBS + glutamine media to promote growth in U937 macrophages with CFU plating on CYET plates, whereas pMME2400 (+*thyA*) was added to *L. pneumophila* strains by electroporation before growth in *A. castellanii* with selection on CYE plates. For U937 macrophage experiments the control strain was Lp02. For *A. castellanii* experiments that control strain was MML854 (Lp02 + pMME2400, G->A mutation at chromosome position 2134550).

**Data availability**

PacBio CCS BAM sequencing files are available at NCBI SRA under BioProject PRJNA902385 (https://www.ncbi.nlm.nih.gov/bioproject/PRJNA902385).

**Acknowledgements**

We thank the members of the Machner lab for thoughtful scientific discussion during the development of the MuRCiS workflow. We thank members of the NIH NICHD Molecular Genomics Core, especially Tianwei Li and James Iben, for executing the Illumina whole genome sequencing, PacBio long-read sequencing, and for performing initial processing and transfer of data files.

**Funding acknowledgement**

This work was funded by the Intramural Research Program of the National Institutes of Health, USA under Project Number 1ZIAHD008893-12 (to M.P.M.) and the Great Lakes Bioenergy Research Center, U.S. Department of Energy, Office of Science, Office of Biological and Environmental Research under Award Number DE-SC0018409 (to T.J.D.).

## References


1. Nowak, M.A., Boerlijst, M.C., Cooke, J. & Smith, J.M. Evolution of genetic redundancy. *Nature* **388**, 167-171 (1997).
2. Ghosh, S. & O'Connor, T.J. Beyond Paralogs: The Multiple Layers of Redundancy in Bacterial Pathogenesis. *Front Cell Infect Microbiol* **7**, 467 (2017).
3. Louca, S. et al. Function and functional redundancy in microbial systems. *Nat Ecol Evol* **2**, 936-943 (2018).
4. Ryan, R.P., Fouhy, Y., Lucey, J.F. & Dow, J.M. Cyclic di-GMP signaling in bacteria: recent advances and new puzzles. *J Bacteriol* **188**, 8327-8334 (2006).
5. Levi, A., Folcher, M., Jenal, U. & Shuman, H.A. Cyclic diguanylate signaling proteins control intracellular growth of *Legionella pneumophila*. *MBio* **2**, e00316-00310 (2011).
6. Römling, U., Galperin, M.Y. & Gomelsky, M. Cyclic di-GMP: the first 25 years of a universal bacterial second messenger. *Microbiol Mol Biol Rev* **77**, 1-52 (2013).
7. McCarty, N.S., Graham, A.E., Studená, L. & Ledesma-Amaro, R. Multiplexed CRISPR technologies for gene editing and transcriptional regulation. *Nature Communications* **11**, 1281 (2020).
8. Adiego-Perez, B. et al. Multiplex genome editing of microorganisms using CRISPR-Cas. *FEMS Microbiol Lett* **366** (2019).
9. Gasiunas, G., Barrangou, R., Horvath, P. & Siksnys, V. Cas9-crRNA ribonucleoprotein complex mediates specific DNA cleavage for adaptive immunity in bacteria. *Proc Natl Acad Sci U S A* **109**, E2579-2586 (2012).
10. Hille, F. et al. The Biology of CRISPR-Cas: Backward and Forward. *Cell* **172**, 1239-1259 (2018).
11. Jinek, M. et al. A programmable dual-RNA-guided DNA endonuclease in adaptive bacterial immunity. *Science* **337**, 816-821 (2012).
12. Adli, M. The CRISPR tool kit for genome editing and beyond. *Nat Commun* **9**, 1911 (2018).
13. Qi, L.S. et al. Repurposing CRISPR as an RNA-guided platform for sequence-specific control of gene expression. *Cell* **152**, 1173-1183 (2013).
14. Vigouroux, A. & Bikard, D. CRISPR Tools To Control Gene Expression in Bacteria. *Microbiol Mol Biol Rev* **84** (2020).
15. Peters, J.M. et al. A Comprehensive, CRISPR-based Functional Analysis of Essential Genes in Bacteria. *Cell* **165**, 1493-1506 (2016).
16. Peters, J.M. et al. Enabling genetic analysis of diverse bacteria with Mobile-CRISPRi. *Nat Microbiol* **4**, 244-250 (2019).
17. Ellis, N.A., Kim, B., Tung, J. & Machner, M.P. A multiplex CRISPR interference tool for virulence gene interrogation in *Legionella pneumophila*. *Commun Biol* **4**, 157 (2021).
18. Liao, C. et al. Modular one-pot assembly of CRISPR arrays enables library generation and reveals factors influencing crRNA biogenesis. *Nat Commun* **10**, 2948 (2019).
19. Cress, B.F. et al. CRISPathBrick: Modular Combinatorial Assembly of Type II-A CRISPR Arrays for dCas9-Mediated Multiplex Transcriptional Repression in *E. coli*. *ACS Synth Biol* **4**, 987-1000 (2015).
20. Hawkins, J.S., Wong, S., Peters, J.M., Almeida, R. & Qi, L.S. Targeted Transcriptional Repression in Bacteria Using CRISPR Interference (CRISPRi). *Methods Mol Biol* **1311**, 349-362 (2015).

21. Vad-Nielsen, J., Lin, L., Bolund, L., Nielsen, A.L. & Luo, Y. Golden Gate Assembly of CRISPR gRNA expression array for simultaneously targeting multiple genes. *Cell Mol Life Sci* **73**, 4315-4325 (2016).
22. Deaner, M., Holzman, A. & Alper, H.S. Modular Ligation Extension of Guide RNA Operons (LEGO) for Multiplexed dCas9 Regulation of Metabolic Pathways in Saccharomyces cerevisiae. *Biotechnol J* **13**, e1700582 (2018).
23. Zuckermann, M. et al. A novel cloning strategy for one-step assembly of multiplex CRISPR vectors. *Sci Rep* **8**, 17499 (2018).
24. McCarty, N.S., Shaw, W.M., Ellis, T. & Ledesma-Amaro, R. Rapid Assembly of gRNA Arrays via Modular Cloning in Yeast. *ACS Synth Biol* **8**, 906-910 (2019).
25. Shaw, W.M. et al. Inducible expression of large gRNA arrays for multiplexed CRISPRai applications. *Nat Commun* **13**, 4984 (2022).
26. McDade, J.E. et al. Legionnaires' disease: isolation of a bacterium and demonstration of its role in other respiratory disease. *N Engl J Med* **297**, 1197-1203 (1977).
27. Fraser, D.W. et al. Legionnaires' disease: description of an epidemic of pneumonia. *N Engl J Med* **297**, 1189-1197 (1977).
28. Burstein, D. et al. Genomic analysis of 38 *Legionella* species identifies large and diverse effector repertoires. *Nat Genet* **48**, 167-175 (2016).
29. Gomez-Valero, L. et al. More than 18,000 effectors in the Legionella genus genome provide multiple, independent combinations for replication in human cells. *Proc Natl Acad Sci U S A* **116**, 2265-2273 (2019).
30. Ensminger, A.W. & Isberg, R.R. *Legionella pneumophila* Dot/Icm translocated substrates: a sum of parts. *Curr Opin Microbiol* **12**, 67-73 (2009).
31. Mondino, S. et al. Legionnaires' Disease: State of the Art Knowledge of Pathogenesis Mechanisms of Legionella. *Annu Rev Pathol* **15**, 439-466 (2020).
32. Chauhan, D. & Shames, S.R. Pathogenicity and Virulence of *Legionella*: Intracellular replication and host response. *Virulence* **12**, 1122-1144 (2021).
33. O'Connor, T.J., Adepoju, Y., Boyd, D. & Isberg, R.R. Minimization of the *Legionella pneumophila* genome reveals chromosomal regions involved in host range expansion. *Proc Natl Acad Sci U S A* **108**, 14733-14740 (2011).
34. Shames, S.R. et al. Multiple *Legionella pneumophila* effector virulence phenotypes revealed through high-throughput analysis of targeted mutant libraries. *Proc Natl Acad Sci U S A* **114**, E10446-E10454 (2017).
35. Zimmermann, L. et al. A Completely Reimplemented MPI Bioinformatics Toolkit with a New HHpred Server at its Core. *J Mol Biol* **430**, 2237-2243 (2018).
36. Krogh, A., Larsson, B., von Heijne, G. & Sonnhammer, E.L. Predicting transmembrane protein topology with a hidden Markov model: application to complete genomes. *J Mol Biol* **305**, 567-580 (2001).
37. Belyi, Y., Tabakova, I., Stahl, M. & Aktories, K. Lgt: a family of cytotoxic glucosyltransferases produced by *Legionella pneumophila*. *J Bacteriol* **190**, 3026-3035 (2008).
38. Wexler, M., Zusman, T., Linsky, M., Lifshitz, Z. & Segal, G. The *Legionella* genus core effectors display functional conservation among orthologs by themselves or combined with an accessory protein. *Curr Res Microb Sci* **3**, 100105 (2022).

39. Isaac, D.T., Laguna, R.K., Valtz, N. & Isberg, R.R. MavN is a *Legionella pneumophila* vacuole-associated protein required for efficient iron acquisition during intracellular growth. *Proc Natl Acad Sci U S A* **112**, E5208-5217 (2015).
40. Christenson, E.T. et al. The iron-regulated vacuolar *Legionella pneumophila* MavN protein is a transition-metal transporter. *Proc Natl Acad Sci U S A* **116**, 17775-17785 (2019).
41. Coers, J. et al. Identification of Icm protein complexes that play distinct roles in the biogenesis of an organelle permissive for *Legionella pneumophila* intracellular growth. *Mol Microbiol* **38**, 719-736 (2000).
42. Park, J.M., Ghosh, S. & O'Connor, T.J. Combinatorial selection in amoebal hosts drives the evolution of the human pathogen *Legionella pneumophila*. *Nature Microbiology* **5**, 599-609 (2020).
43. Feeley, J.C. et al. Charcoal-yeast extract agar: primary isolation medium for *Legionella pneumophila*. *J Clin Microbiol* **10**, 437-441 (1979).
44. Schmittgen, T.D. & Livak, K.J. Analyzing real-time PCR data by the comparative C(T) method. *Nat Protoc* **3**, 1101-1108 (2008).
45. Moffat, J.F. & Tompkins, L.S. A quantitative model of intracellular growth of *Legionella pneumophila* in *Acanthamoeba castellanii*. *Infect Immun* **60**, 296-301 (1992).
46. Li, H. et al. The Sequence Alignment/Map format and SAMtools. *Bioinformatics* **25**, 2078-2079 (2009).
47. Wibawa, R.R., Li, P., McCaffrey, K. & Hartland, E.L. Using Genomic Deletion Mutants to Investigate Effector-Triggered Immunity During *Legionella pneumophila* Infection. *Methods Mol Biol* **2523**, 23-41 (2022).
48. Lee, P.C. & Machner, M.P. The *Legionella* Effector Kinase LegK7 Hijacks the Host Hippo Pathway to Promote Infection. *Cell Host Microbe* **24**, 429-438.e426 (2018).

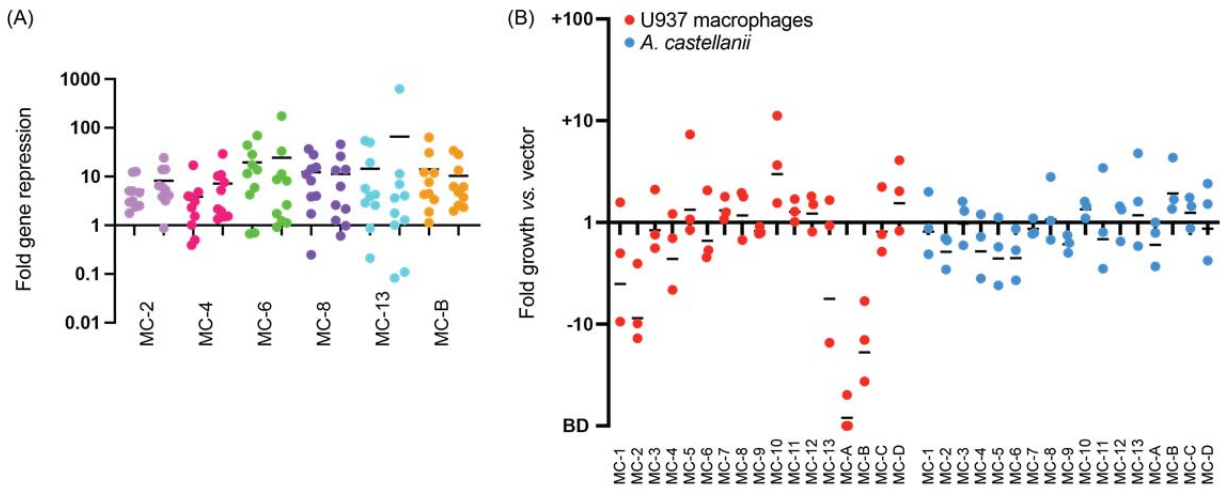


**Figure 1: Intracellular growth of Lp02(*dcas9*) upon CRISPRi gene silencing with pre-determined 10-plex arrays**

(A) Gene silencing efficiency assay. Each of the ten genes targeted by one of the six indicated MC arrays was assayed for gene repression by qPCR. RNA levels in the Lp02(*dcas9*) strain bearing the CRISPR array were compared to that bearing an empty vector. Data are a summary of two replicates shown side-by-side. Horizontal bars indicate mean fold repression of all targets of the array. (B) *L. pneumophila* intracellular growth assay. Host cells were challenged at a multiplicity of infection (MOI) of 0.05 (U937 macrophages) or 0.03 (*A. castellanii*) with Lp02(*dcas9*) bearing the indicated MC arrays. Colony forming units (CFUs) of samples taken 2 hours post infection (hpi) and either 72 (U937 macrophages) or 48 (*A. castellanii*) hpi were determined, and fold growth of Lp02(*dcas9*) bearing the indicated MC arrays relative to that of Lp02(*dcas9*) bearing the empty vector was plotted. Numbers below 1 indicate a growth defect upon gene silencing. BD, below detection (arbitrarily set to -100). Horizontal bars indicate mean fold growth *vs.* vector using data from three replicates.

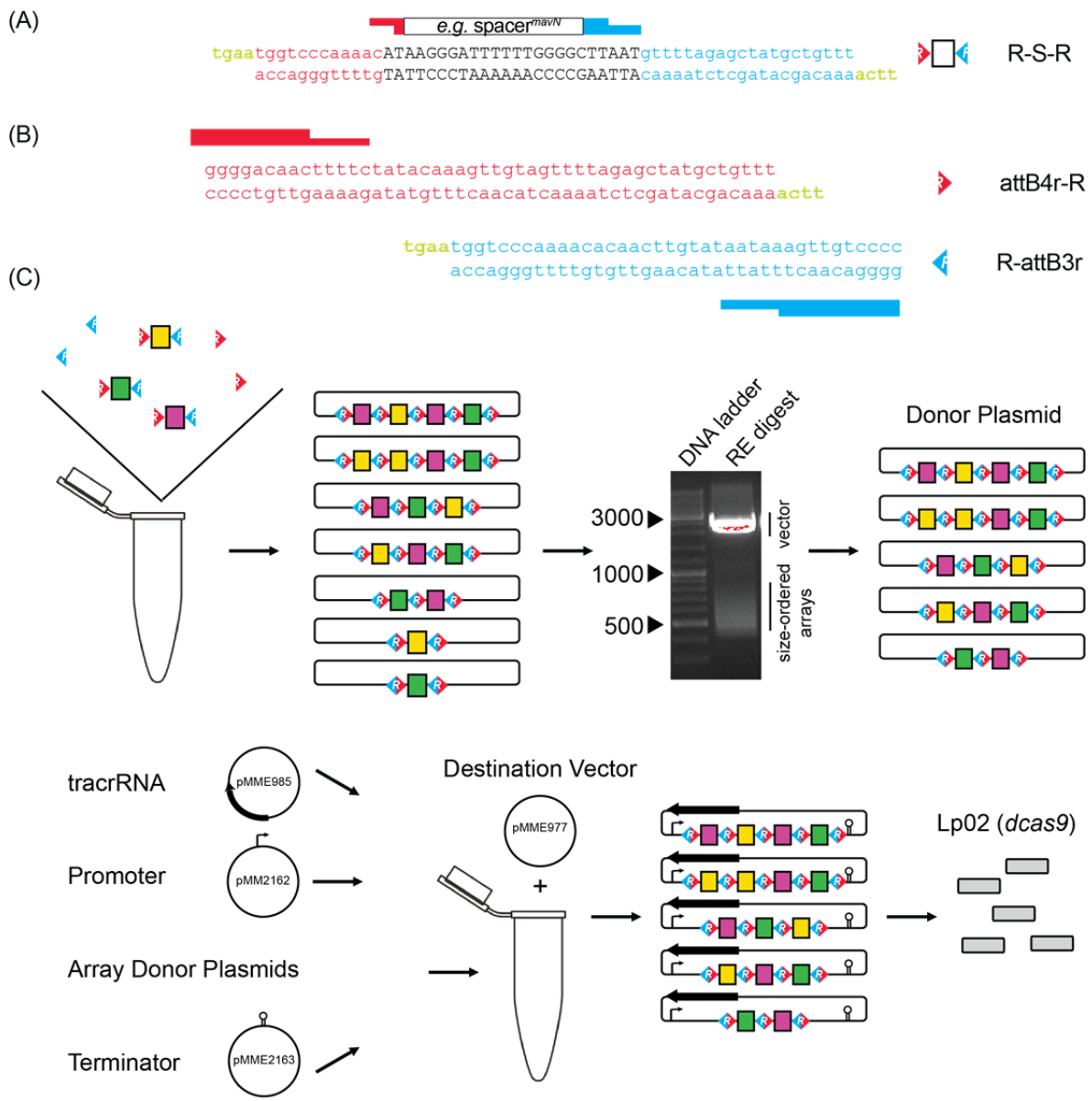


809

810 **Figure 2: Cloning strategy for *de novo* self-assembly of CRISPR array libraries**

811 (A) Nucleotide sequence of R-S-R building blocks. Each R-S-R element is composed of a top

812 and bottom oligonucleotide. The 24 bp spacer sequence (black font; shown for crRNA$^{mavN}$ as an

813 example) is flanked by sequences of the upstream (red) and downstream (blue) repeat element,

814 with each end containing sticky overhangs (green). (B) Nucleotide sequence of attB4r-R and R-

815 attB3r "dead ends" with only one sticky overhang each (green). (C) Array self-assembly, size

816 selection, and cloning. R-S-Rs and “dead end” elements were allowed to self-assemble in a
817 single tube and then ligated together and incorporated into an interim cloning vector. Arrays
818 excised from an interim cloning vector were subjected to gel electrophoresis to separate them
819 according to size. RE, restriction enzyme. After gel extraction, arrays of 550-650 bps and 650-
820 800 bps in size were cloned into a donor plasmid such that three additional elements, namely the
821 tracrRNA, a *tet* promoter, and a *rrnB* T1 terminator, could assemble with the arrays into the
822 destination vector by Invitrogen Multisite Gateway Pro cloning. Final constructs were introduced
823 into Lp02(*dcas9*) by electroporation.

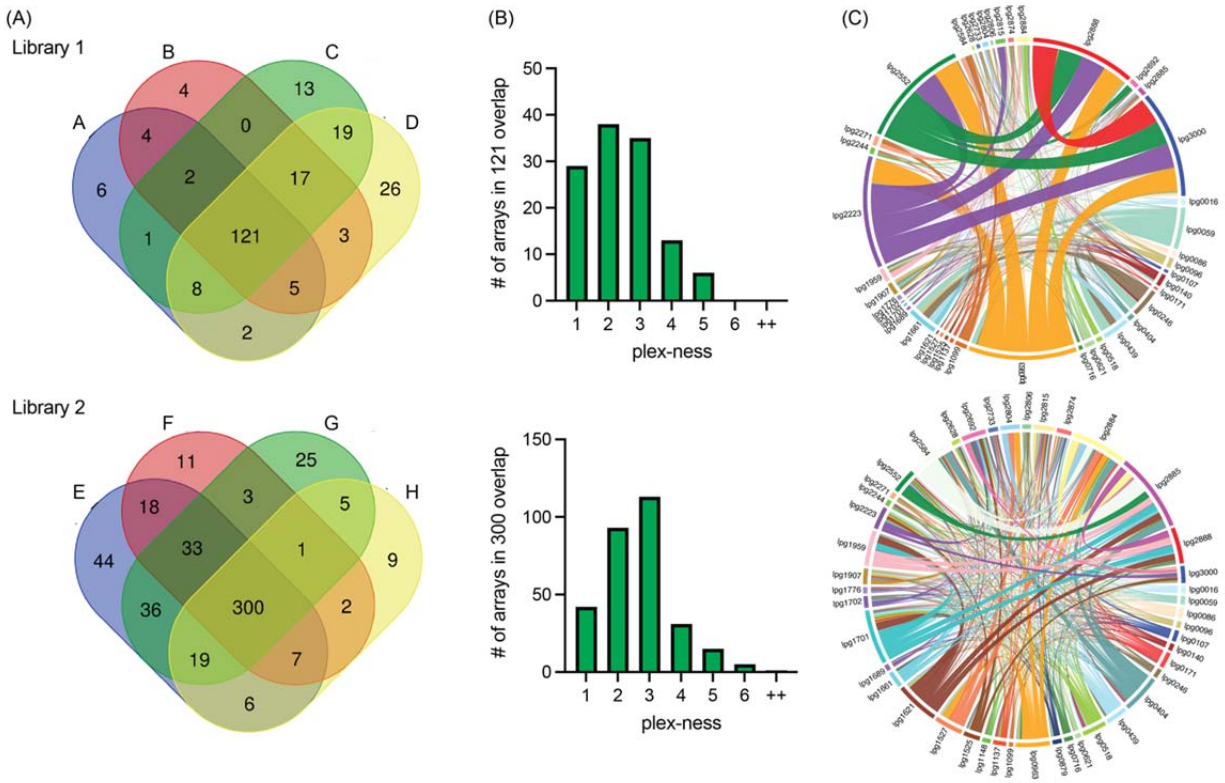


824

825 **Figure 3: Self-assembled CRISPR arrays are diverse in length and spacer composition**

826 (A) Two CRISPR array libraries were built from 44 R-S-R building blocks. Vectors from each

827 library were harvested four times and sequenced. Venn diagrams show the overlap of unique

828 spacer combinations, with the requirement of five or more raw (pre-sequence-depth normalized)

829 read counts per array in each round of sequencing. (B) The distribution of plex-ness (spacer

830 count) for arrays found in all four rounds of sequencing. (C) Chord diagrams link TME genes,

831 listed around the outside of the circle, each time spacers targeting each is present in an array.

832 Link line width is weighted according to the number of times the combination of spacers was

833 observed. Link line color is unique for each spacer and is constant between the two diagrams.

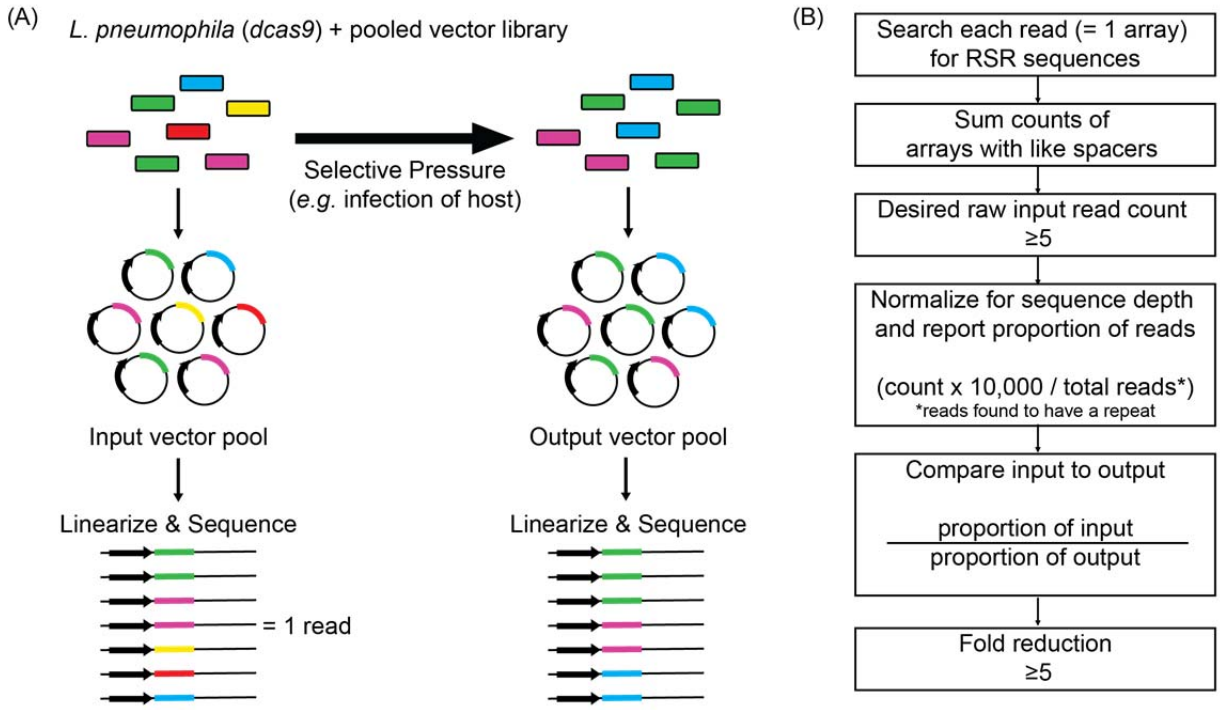


**Figure 4: Schematic overview of the experimental and bioinformatics pipeline of MuRCiS** (A) During MuRCiS, a pooled population of *L. pneumophila* (*dcas9*) bearing the multiplex random CRISPR arrays were subjected to a selective pressure (intracellularity). Vectors were purified from both input and output bacteria populations, linearized, and submitted for long-read PacBio Sequel sequencing. For simplification, an array of mixed spacer population is shown as a single stretch of color, each color representing a different combination of spacers. In this example, the yellow and red arrays are lost in the output suggesting they silence critical combinations of genes. (B) Overview of the custom bioinformatics pipeline used to identify unique spacer combinations causing growth attenuation as defined by a fold reduction of five or more (https://github.com/GLBRC/MuRCiS_pipeline).

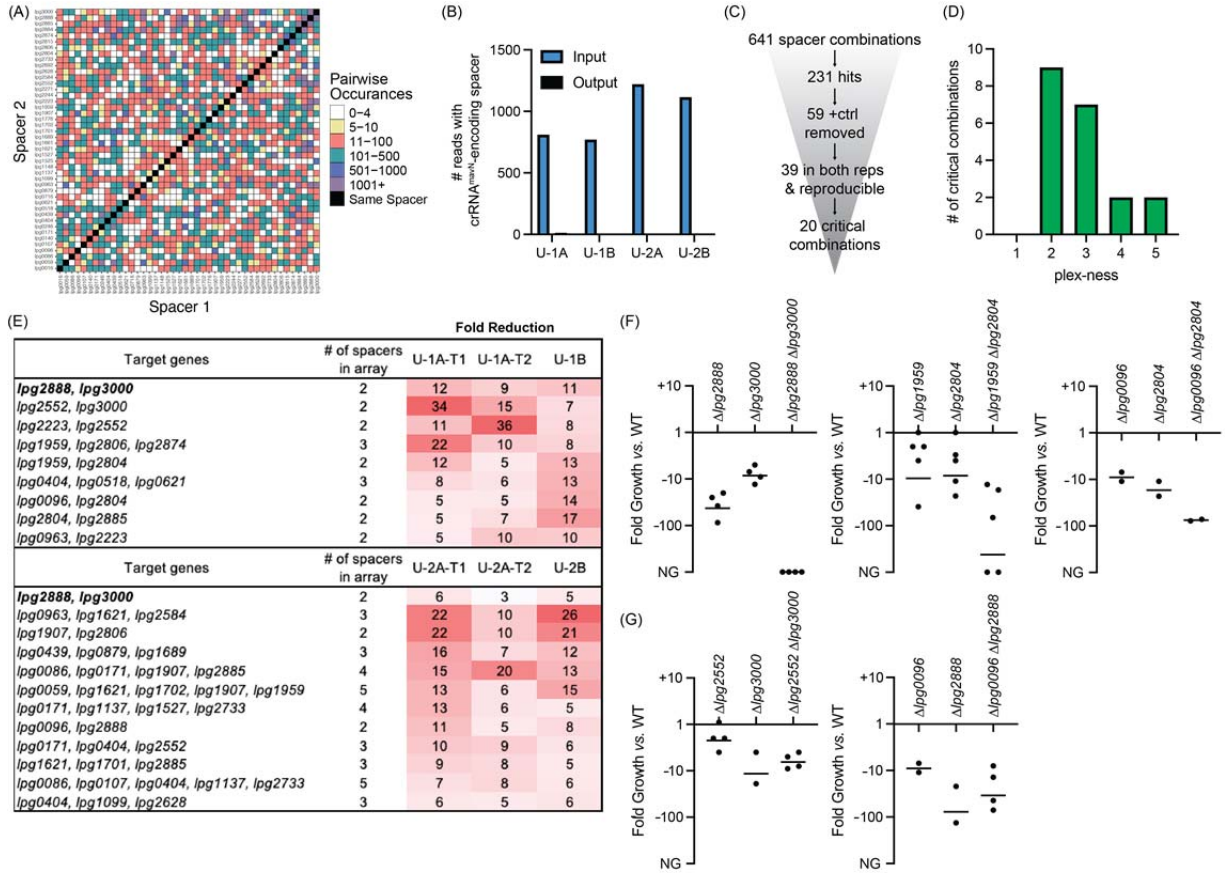


| Target genes | # of spacers in array | U-1A-T1 | U-1A-T2 | U-1B |
|---|---|---|---|---|
| ***lpg2888, lpg3000*** | 2 | 12 | 9 | 11 |
| *lpg2552, lpg3000* | 2 | 34 | 15 | 7 |
| *lpg2223, lpg2552* | 2 | 11 | 36 | 8 |
| *lpg1959, lpg2806, lpg2874* | 3 | 22 | 10 | 8 |
| *lpg1959, lpg2804* | 2 | 12 | 5 | 13 |
| *lpg0404, lpg0518, lpg0621* | 3 | 8 | 6 | 13 |
| *lpg0096, lpg2804* | 2 | 5 | 5 | 14 |
| *lpg2804, lpg2885* | 2 | 5 | 7 | 17 |
| *lpg0963, lpg2223* | 2 | 5 | 10 | 10 |

| Target genes | # of spacers in array | U-2A-T1 | U-2A-T2 | U-2B |
|---|---|---|---|---|
| ***lpg2888, lpg3000*** | 2 | 6 | 3 | 5 |
| *lpg0963, lpg1621, lpg2584* | 3 | 22 | 10 | 26 |
| *lpg1907, lpg2806* | 2 | 22 | 10 | 21 |
| *lpg0439, lpg0879, lpg1689* | 3 | 16 | 7 | 12 |
| *lpg0086, lpg0171, lpg1907, lpg2885* | 4 | 15 | 20 | 13 |
| *lpg0059, lpg1621, lpg1702, lpg1907, lpg1959* | 5 | 13 | 6 | 15 |
| *lpg0171, lpg1137, lpg1527, lpg2733* | 4 | 13 | 6 | 5 |
| *lpg0096, lpg2888* | 2 | 11 | 5 | 8 |
| *lpg0171, lpg0404, lpg2552* | 3 | 10 | 9 | 6 |
| *lpg1621, lpg1701, lpg2885* | 3 | 9 | 8 | 5 |
| *lpg0086, lpg0107, lpg0404, lpg1137, lpg2733* | 5 | 7 | 8 | 6 |
| *lpg0404, lpg1099, lpg2628* | 3 | 6 | 5 | 6 |

**Figure 5: Discovery of *L. pneumophila* gene combinations critical for growth in U937 macrophages**

(A) Correlation grid plotting all pairwise spacer combinations. The number of times two unique spacers were present in the sequenced array library is indicated by color-coding, ranging from light (rare) to dark (abundant). Black boxes, same spacer. (B) Total number of reads bearing the spacer which encodes crRNA$^{mavN}$. Counts in technical output replicates were summed. (C) Flow-chart going from the number of total spacer combinations to the number of critical combinations identified. (D) Histogram indicating the plex-ness of all critical spacer combinations identified. (E) A list of virulence-critical combinations of genes and the corresponding fold reduction observed for each in each experiment. Library 1 results are shown above Library 2 results. (F) Intracellular growth assays of strains with deletions in the indicated genes. Results are given as

857 fold growth (CFUs harvested 72 hpi *vs.* 2 hpi) compared to that of Lp02 (WT). Horizontal bars
858 indicate mean fold growth of the deletion strain *vs.* WT strain for two or more experimental
859 replicates. NG, no growth (arbitrarily set to -1000). (G) Intracellular growth assays of deletion
860 strains that do not have a synergistic phenotype.

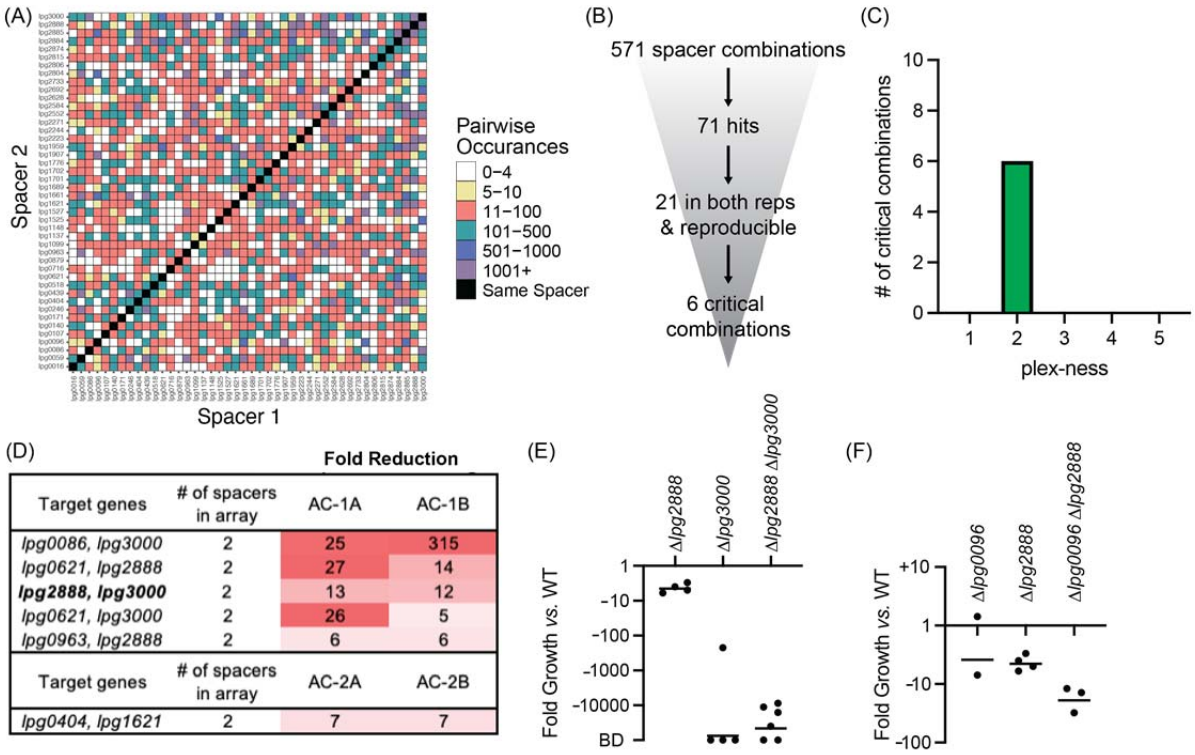


| Target genes | # of spacers in array | AC-1A | AC-1B |
|---|---|---|---|
| *lpg0086, lpg3000* | 2 | 25 | 315 |
| *lpg0621, lpg2888* | 2 | 27 | 14 |
| ***lpg2888, lpg3000*** | 2 | 13 | 12 |
| *lpg0621, lpg3000* | 2 | 26 | 5 |
| *lpg0963, lpg2888* | 2 | 6 | 6 |

| Target genes | # of spacers in array | AC-2A | AC-2B |
|---|---|---|---|
| *lpg0404, lpg1621* | 2 | 7 | 7 |

**Figure 6: Discovery of *L. pneumophila* gene combinations critical for growth in *A. castellanii***

(A) Correlation grid plotting all pairwise spacer combinations. The number of times two unique spacers were present in the sequenced array library is indicated by color-coding, ranging from light (rare) to dark (abundant). Black boxes, same spacer. (B) Flow-chart going from the number of total spacer combinations to the number of critical combinations identified. (C) Histogram indicating the plex-ness of all critical spacer combinations identified. (D) A list of virulence-critical combinations of genes and the corresponding fold reduction observed for each in each experiment. Library 1 results are shown above Library 2 results. (E) Intracellular growth assays of strains +pMME2400 with deletions in the indicated genes. Results are given as fold growth (CFUs harvested 48 hpi *vs.* 2 hpi) compared to that of Lp02 +pMME2400 (WT). Horizontal bars indicate mean fold growth of the deletion strain *vs.* WT strain for two or more experimental

874 replicates. BD, below detection (arbitrarily set to -100,000). (F) Intracellular growth assays of
875 strains with deletions in the indicated genes having been identified in single-round CRISPRi
876 experiments.

**Supplemental Information**

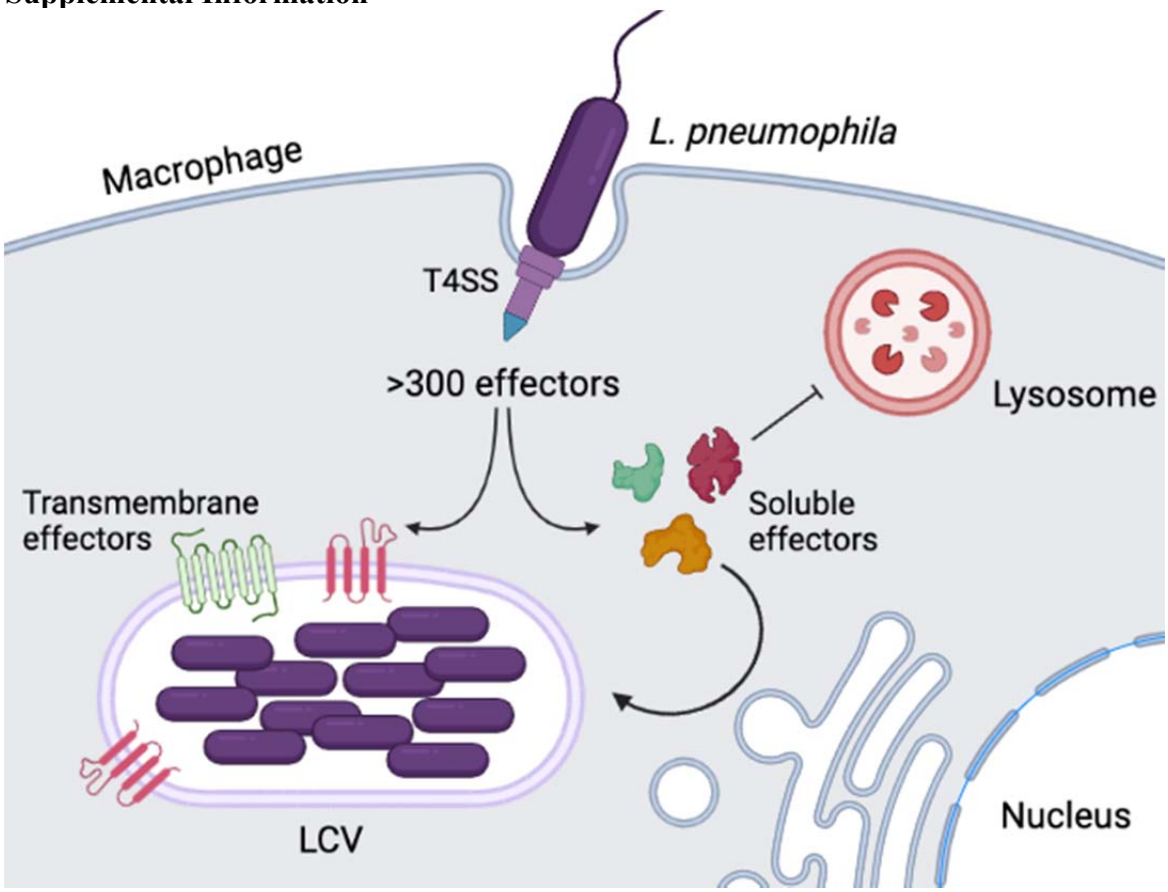


**Figure S1: Model of the *Legionella*-containing vacuole bearing transmembrane effectors.** *L. pneumophila* translocates >300 effector proteins *via* a T4SS into a host cell to re-wire cellular pathways to evade the lysosome and establish a replication vacuole known as the *Legionella*-containing vacuole (LCV). It is hypothesized that transmembrane effectors are incorporated into the LCV for nutrient acquisition, detoxification, and membrane fusion. Diagram made using BioRender (https://biorender.com).

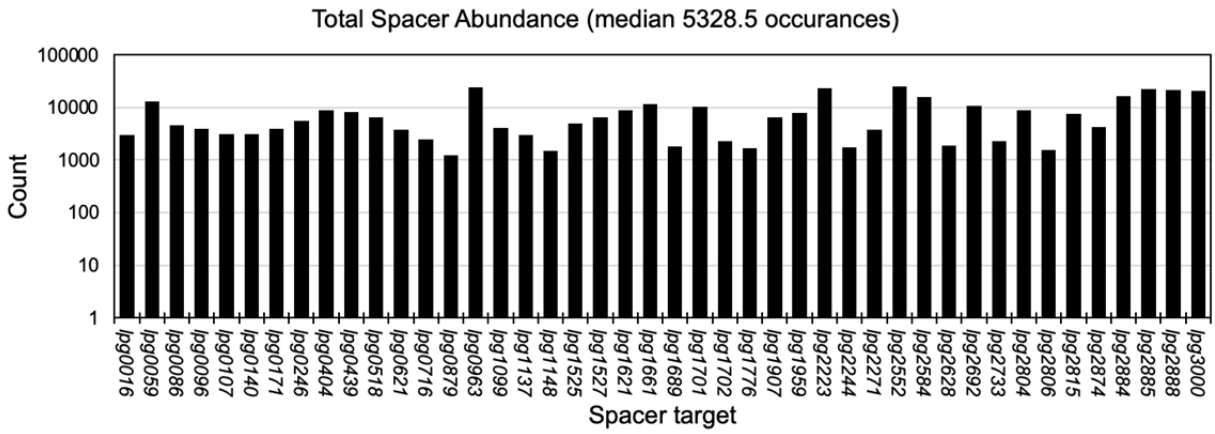


**Figure S2: Spacer abundance post CRISPRi induction.**

The occurrence of each spacer within the plasmid libraries was quantified 24 hours post induction of expression. The fact that each spacer was well represented within the library indicated that the crRNA products of these spacers were not toxic to axenic *L. pneumophila* growth.

**Note S1: *In vitro* CRISPR array assembly**

The *in vitro* assembly of crRNA-encoding arrays is a key accomplishment of our approach. While it seems simple on paper, the actual assay proved to be technically demanding and required various optimization steps. For experimenters interested in applying our technology to their own research question, the following is a list of strategies we also tried:

**Size selection of CRISPR arrays:** To enrich for longer CRISPR arrays, we explored use of size-selection SPRI beads (Beckman), Pippin Prep instrumentation (Sage Science), and immediate purification from the R-S-R assembly mix by DNA gel electrophoresis. The goal was to maintain the most ligated material and give preference to longer arrays that are outcompeted by smaller arrays during vector incorporation. While these approaches were able to size-select for longer arrays, the highest yield of size-selected arrays occurred when the ligated arrays were first

introduced into an interim plasmid, then excised *via* restriction enzyme digest, size-ordered by gel electrophoresis, extracted from the gel, and then ligated back into the donor plasmid.

**Addition of promoter and terminator:** Attempts to add dead ends bearing the promoter and terminator sequences to the original R-S-R assembly mix led to muddled array assembly which we believed to be the result of the promoter and terminator fragments being much longer (~200 bps) than the R-S-R building blocks (60 bps) Therefore, addition of the promoter and terminator to the final plasmid was accomplished by Invitrogen Multisite Gateway Pro cloning as described.

**Barcoding of arrays:** Barcodes are often used to distinguish between different constructs in library-based experiments. The pooled nature of our *de novo* array self-assembly protocol thwarts unique barcode addition without interim isolation of each array followed by long-read sequencing to assign each array to a unique bar code. Since long-read sequencing by PacBio sequences each array in its entirety, our MuRCiS pipeline negates the need for barcodes altogether.

**Sub-optimal annealing sites:** During the development of our MuRCiS workflow, we also made an array library in which we intentionally designed spacers to encode crRNAs that would target sequences adjacent PAMs further downstream of the transcriptional start site. We hoped they would serve as good off-targeting controls. However, upon performing the infection experiment, we found almost none of the hits that emerged while using the most optimal spacers (Figures 5 and 6) and so we would recommend only using the best crRNA target.

**Supplemental Tables**

Table S1: 10-plex Construct Descriptions and Spacer Sequences

Table S2: TME Genes and Corresponding Spacer Sequences

Table S3: PacBio Long-read Sequencing Metrics

Table S4: Read Counts and Calculations for all Constructs from all Experiments

Table S5: Subset data for all hits identified in U937 macrophage infection experiments

Table S6: Subset data for all critical gene combinations identified in U937 macrophage infection experiments

Table S7: Subset data for all hits identified in *A. castellanii* infection experiments

Table S8: Subset data for all critical gene combinations identified in *A. castellanii* infection experiments

Table S9: Hits found in single round CRISPRi experiments

Table S10: Strains and Plasmids Used in this Study